

ANALYSIS OF ROD REMOVAL TRANSIENT EXPERIMENTS IN VVER REACTORS AT ZERO POWER

Felix C. Difilippo
Oak Ridge National Laboratory
P.O. Box 2008, Oak Ridge, TN 37831-6363 USA
fcd@ornl.gov

ABSTRACT

Within the context of the Fissile Materials Disposition Program of the U.S. Department of Energy we analyzed rod removal transient experiments performed at the Kurchatov Institute in a full-scale mockup of VVER reactors. The transients were started (via water inlet) in slightly (few cents) supercritical configurations with all the control rods withdrawn. After a few minutes, control rods banks or individual control rods were first inserted and later withdrawn (returning to the initial state). Available experimental data include the relative time profiles of nine incore and excore detectors. Because of the mild nature of the transients (very low power and no more than 2 \$ reactivities) we decided to use a quasistatic approach. The time-dependent flux is factorized into two terms: a function of phase space, given by the solution of the static equation with parametric excitation; and a function of time, given by the solution of the point kinetic equations with time-dependent kinetics parameters. Due to the nature of the experiment, cold conditions, control rods withdrawn and critical state with water level, the power distributions, measured and calculated, are quite unusual, with the inner part of the core heavily shielded. Measured power levels at the center of the reactor are almost 20 times smaller than similar regions at the periphery. Transport and diffusion calculations of the power distributions are in reasonable agreement, so the diffusion code BOLD-VENTURE was used to calculate the kinetics parameters and the relative changes of the detector field of view. The numerical integration of the time-dependent part of the solution was made with the LSODE package using ENDF/B-V and VI delayed neutron data. Very good results were obtained for the nine time profiles.

1. INTRODUCTION

The governments of the United States (US) and the Russian Federation (RF) have agreed to dispose of surplus, weapons-usable plutonium by irradiating the material in commercial, pressurized-water, power reactors—designated as VVERs in the RF. As in the US, in the RF, it must be demonstrated to regulatory authorities that VVERs can be operated with a sufficient level of safety when approximately one-third of the reactor core is composed of mixed-oxide (MOX)-fueled assemblies.

Since 1997, staff at the Oak Ridge National Laboratory (ORNL) have served as independent reviewers for VVER MOX analyses performed in the RF. Past studies have included the validation of computer programs with critical experiment data and the design of a prototypic VVER MOX assembly. The next stage of analysis concerns the study of anticipated transients. One transient likely to have a large reactivity effect is an unplanned control rod withdrawal incident. Planned VVER MOX fuel management schemes call for only low-enriched-uranium (LEU) assemblies to be placed in control rod locations. In order to validate American reactor physics methods for analyzing an unplanned withdrawal transient, the RF has provided a description of a control rod withdrawal experiment performed with LEU fuel. We analyzed zero-power transients measured¹ at the B-1000 test facility of the Russian Research Center, Kurchatov Institute, in a mock-up of the VVER-1000 power reactor at the beginning of the first loading. The reactor of the experiment had a core composed of 163 hexagonal fuel assemblies of different enrichments (1.6, 3.0, 4.23, and 4.4 wt %). Each assembly contains 312 fuel rods, 18 guide tubes for control rods or burnable poison, and 1 instrument tube. The active height of the core is 353 cm, and the equivalent radius, 158.2 cm.

Seven incore detectors and two excore ionization chambers followed the flux transients; the nine time profiles (normalized to one at the beginning of the transient) are the subject of this analysis. The transient analyzed started in a slightly supercritical system ($\beta \sim +6$ cents) with all control rods withdrawn, boric acid concentration at 8.5 g/L and water level at 237 cm. At $t \sim 300$ s, control rod bank (No. 9) was introduced 100% ($\beta \sim -1.5$); at $t \sim 480$ s, the control rod bank was then totally withdrawn. The transient was recorded until $t \sim 880$ s, and the movements of the rods involved ~ 40 s.

2. MODELING THE TRANSIENTS

Because we have to model mild zero-power transients, we decided to use a quasistatic approach typically used, for example, to calibrate control rods via the inverse kinetics methods. The next sections present the method and its implementation.

2.1 QUASISTATIC REACTOR KINETICS

The quasistatic approximation is described, for example, in Ref. 2. We can arbitrarily factorize the flux as

$$\phi(\vec{\mu}, t) = \psi(\vec{\mu}, t)h(t) \quad , \quad (1)$$

where $\vec{\mu} = (\vec{r}, \vec{v})$ is the position of the neutrons in phase space at time, t , and h is a function of time only. The quasistatic approximation of ψ is the solution of the static balance equation

$$\left[-\hat{D}(t) + \chi_s \frac{\hat{P}(t)}{k(t)} \right] \psi = 0 \quad , \quad (2)$$

where the destruction, \hat{D} , and production, \hat{P} , operators are explicitly functions of time because of the parametric excitation of the reactor, $k(t)$ is the static eigenvalue and χ_s is the static fission spectrum. After solving Eq. (2) in direct and adjoint spaces, it follows that, provided the calculations are normalized to the same neutron production rate, the time factor $h(t)$ is given by $n = h \Lambda(t)/\Lambda(0)$, where $n(t)$ is given by the solution of the point kinetic equations.

The normalized reaction rate of detector, d , is given then by

$$Q_d(t) \equiv \frac{I_d(t)}{I_d(0)} = \frac{\langle \sum_d \psi(t) \rangle_d}{\langle \sum_d \psi(0) \rangle_d} n(t) \frac{\Lambda(0)}{\Lambda(t)} \quad , \quad (3)$$

where the integrals in phase space are restricted to the volume of the detector, d . The solution is completed with the step-by-step solution of the point-kinetics equation (all kinetics parameters are defined in the next two paragraphs):

$$\begin{aligned} \frac{dn}{dt} &= \frac{\beta - 1}{\Lambda^*} n + \sum_{i=1}^I \sum_{g=1}^G \lambda_g^i C_g^i \\ \frac{dC_g^i}{dt} &= b_g^i \frac{n}{\Lambda^*} - \lambda_g^i C_g^i \quad , \end{aligned} \quad (4)$$

where i , is the index of I fissile isotopes, and g is the index for the corresponding delayed neutron groups. The now time-dependent kinetics parameters are the reduced generation time,

$$\Lambda^*(t) = l/k\beta_{ef} \quad ; \quad (5)$$

the neutron mean life,

$$l(t) = \frac{\left\langle \Psi^+ \left| \frac{1}{v} \Psi \right. \right\rangle}{\left\langle \Psi^+ \left| \hat{D}(t) \Psi \right. \right\rangle} \quad ; \quad (6)$$

the delayed neutron effectiveness,

$$\gamma_g^i = \frac{\left\langle \Psi^+ \left| \chi_g^i \hat{P}_i \Psi \right. \right\rangle}{\left\langle \Psi^+ \left| \chi_s \hat{P} \Psi \right. \right\rangle} \quad ; \quad (7)$$

the reactivity in dollar units,

$$\$(t) = \frac{k(t) - 1}{k(t)\beta_{ef}} \quad ; \quad (8)$$

and the effective delayed neutron fraction;

$$\beta_{ef} = \sum_{i=1}^I \sum_{g=1}^G \gamma_g^i \beta_g^i \quad . \quad (9)$$

In the previous equations, the production operator $\hat{P} = \sum_{i=1}^I \hat{P}_i$ is a sum over the fissile species, and the static fission spectrum is $\chi_s = \sum_{i=1}^I \chi_s^i \hat{P}_i \Psi / \sum_{i=1}^I \hat{P}_i \Psi$, where $\chi_s^i = \chi_p^i (1 - \beta^i) + \sum_{g=1}^G \beta_g^i \chi_g^i$ and $\beta^i = \sum_{g=1}^G \beta_g^i$. Parameters β_g^i and χ_g^i are the nuclear fraction and the spectra of the delayed neutron group g of fissile i and χ_p^i its prompt fission spectra. The contribution of the delayed group (i, g) in Eq. (4) is $b_g^i = \beta_{gef}^i / \beta_{ef} = \beta_g^i \gamma_g^i / \beta_{ef}$. The effective delayed neutron fraction, β_{ef} , is the parameter that relates the static k to the experimental dollar unit. For mild transients, the largest variations are for $\$(t)$.

2.2 STEPS FOR THE DEVELOPMENT OF THE QUASISTATIC MODEL

Cross-section libraries for the assemblies were generated in the AMPX³ format for transport and diffusion theory calculations. The number of energy groups were chosen to fit well the spectral differences between prompt and delayed fission neutrons. We used the Helios⁴ code (ENDF/B-VI-based) with a special module to generate P1 AMPX cross sections for each one of the different assemblies with and without control rods. The AMPX system was used to generate P3 cross sections, but with pin, rather than assembly, geometry. Transport calculations of power distributions using DORT⁵ (r, θ geometry) were successfully compared with diffusion-theory (triangular-mesh) values. (See Figure 1 for details.) Note that the cold condition at the beginning of life produces a highly skewed distribution and that the triangular geometry of the diffusion approximation allows a more accurate description of the hexagonal geometry of the core. We concluded

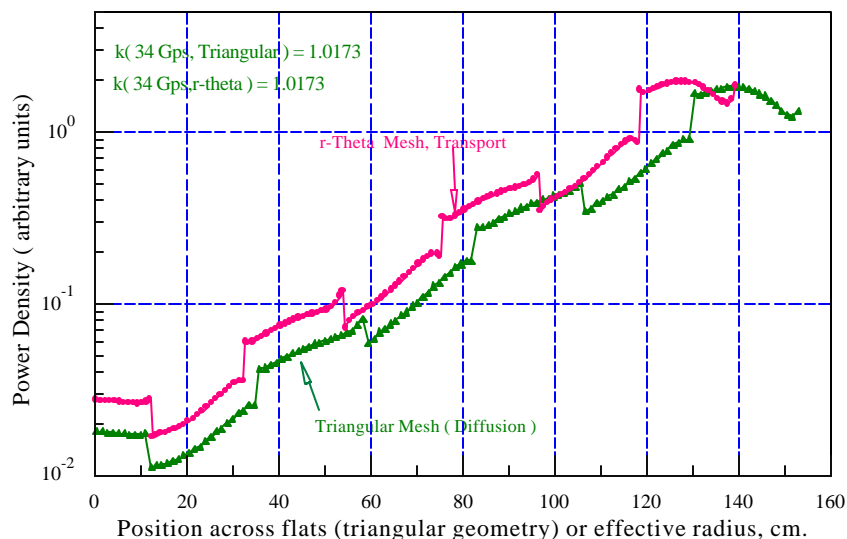


Figure 1. Transport and diffusion theory power distribution.

then that the use of the diffusion-theory BOLD-VENTURE⁶ system in triangular geometry is a good approximation to compute direct and adjoint fluxes necessary to calculate the bilinear averages described in the previous section. Sets of effective kinetics parameters were then calculated based on nuclear data from the compilations of Keepin,⁷ ENDF/B-V and ENDF/B-VI.⁸ Reactivities in absolute units (i.e., in k units) between the two extreme values (totally withdraw and totally inserted) were interpolated with a \cos^2 distribution in z for the intermediate values of the rod position. The transients were finally calculated with the LSODE⁹ ordinary differential equation integrator.

2.3 KINETICS PARAMETERS

Table I shows the nuclear delayed neutron data corresponding to our two fissile species ²³⁵U and ²³⁸U that were used, together with their respective spectra, to perform the bilinear averages of Section 2.1. The effects of the control rod position on the kinetics parameters are summarized in Table II, where it is shown that for this mild transient, generation times and effective delayed neutron fractions change very little. Effective delayed neutron fractions calculated using ENDF/B-V, ENDF/B-VI, and Keepin's nuclear data are shown in Table III. The ~20% difference for the mean emission time of a delayed neutron between the ENDF/B-V and -VI compilations is indicative of the discrepancies between the respective relationships between the reactivity and the period (inhour equation).

Even though columns V and VI in Table 3 were calculated with the prescriptions of Section 2.1 (i.e., with the bilinear averages of direct and adjoint fluxes), the Keepin column was calculated by "hand" using a representative value of 5.46% for the relative fission neutron production in ²³⁸U. Comparison of this column with the others shows that because the system is large it does not show a significant difference between the escape probabilities of prompt and delayed neutron. The betas are then mainly defined by the relative fission distribution between the two uranium isotopes.

Table I. Delayed Neutron Nuclear Data

Group	Relative abundance			Production per fission neutron			
	Keepin	ENDF/B-V	ENDF/B-VI	Keepin	ENDF/B-V	ENDF/B-VI	
²³⁵U Thermal Fission^a							
1	0.033	0.038	0.0350	0.000226	0.00026	0.00024	
2	0.219	0.213	0.1807	0.001501	0.00146	0.001238	
3	0.196	0.188	0.1725	0.001343	0.001288	0.001182	
4	0.395	0.407	0.3868	0.002707	0.002789	0.002651	
5	0.115	0.128	0.1586	0.000788	0.000877	0.001087	
6	0.042	0.026	0.0664	0.000288	0.000178	0.000455	
Total	1.000	1.000	1.0000	0.006854	0.006854	0.006854	
²³⁸U 2.0 MeV Fission^b							
1	0.013	0.013	0.0139	0.000216	0.000216	0.000231	
2	0.137	0.137	0.1128	0.002279	0.002279	0.001877	
3	0.162	0.162	0.1310	0.002695	0.002695	0.002179	
4	0.388	0.388	0.3852	0.006455	0.006455	0.006408	
5	0.225	0.225	0.2540	0.003743	0.003743	0.004226	
6	0.075	0.075	0.1031	0.001248	0.001248	0.001715	
Total	1.000	1.000	1.0000	0.016636	0.016636	0.016636	
Lambda (1/s)							
	²³⁵U				²³⁸U		
Group	Keepin	ENDF/B-V	ENDF/B-VI	Keepin	ENDF/B-V	ENDF/B-VI	
1	0.0124	0.0127	0.0133	0.0132	0.0132	0.01363	
2	0.0305	0.0317	0.0327	0.0321	0.0321	0.03133	
3	0.1110	0.1160	0.1208	0.1390	0.1390	0.12330	
4	0.3010	0.3110	0.3028	0.3580	0.3590	0.32370	
5	1.1400	1.4000	0.8495	1.4100	1.4100	0.90600	
6	3.0100	3.8700	2.8530	4.0200	4.0300	3.04870	

^aNumber of delayed neutrons per fission = 0.0167 (original Keepin data = 0.0158) ; number of neutrons per fission = 2.4367.

^bNumber of delayed neutrons per fission = 0.044 (original Keepin data = 0.0412) ; number of neutron per fission = 2.6448.

Table II. Kinetics Parameters as Function of Control Rod Position^a

	Bank No. 9 out	Bank No. 9 in
Reactivity, $\rho = (k - 1)/k$	Reference state	-1.1961%
Generation Time, $\Lambda = \ell / k(\mu s)$	17.60	17.64
β_{ef} (ENDF/B-V)	0.007416	0.007437
β_{ef} (ENDF/B-VI)	0.007408	0.007428

^aBold-Venture, diffusion calculation, 2-D triangular mesh.

Table III. Effective Delayed Neutron Fractions

i, Fissile specie	g, Delayed group	ENDF/B-V	ENDF/B-VI	Keepin
1, ²³⁵ U	1	2.490E-04	2.333E-04	2.130E-04
	2	1.384E-03	1.175E-03	1.416E-03
	3	1.224E-03	1.122E-03	1.267E-03
	4	2.650E-03	2.512E-03	2.554E-03
	5	8.334E-04	1.031E-03	7.440E-04
	6	1.693E-04	4.319E-04	2.720E-04
2, ²³⁸ U	1	1.182E-05	1.260E-05	1.200E-05
	2	1.237E-04	1.017E-04	1.290E-04
	3	1.464E-04	1.185E-04	1.520E-04
	4	3.514E-04	3.475E-04	3.650E-04
	5	2.039E-04	2.296E-04	2.110E-04
	6	6.797E-05	9.314E-05	7.000E-05
Total		7.416E-03	7.409E-03	7.406E-03
Mean emission	Time (s) ^a	12.13	10.65	12.35

^aMean emission time of a delayed neutron.

3. ANALYSIS OF THE TRANSIENTS

A total of nine detectors followed the transient generated by the insertion and later withdrawals of the bank of control rods No. 9. The reactor had a water level of 237 cm (fuel element length, 353 cm), a concentration of 8.5 g of boric acid per liter of moderator, and a 60° symmetry. The initial state was slightly supercritical (period of 184.5 s) with all the control rods withdrawn. Table IV describes the location of the detectors and the effects of the presence of bank No. 9 in the detector field of view [i.e., the ratio of functional in Eq. (3)].

If the quasistatic approximation is applicable, the ratio of the normalized signals coming from any two detectors, given by Eq. (3), should be equal to 1 before and after the insertion of the rods. This is because the system is returned to the original initial conditions (with the rods withdrawn). Figure 2 shows that this is true even for an extreme case, which corresponds to the ratio of signals from incore detectors 4 and 8 (~ -54% change) divided by the signal from incore detector 7 (~ +30% change).

Table IV. Location of the Detectors and the Effects of Bank No. 9 on Control Rods

Detector name	Location (distance to control rods) ^a	Perturbation of control rod ^b
Incore 1	In next assembly to control rods (1)	0.9075
2	Center of core (6)	1.322
4 and 8	In assembly with control rod (0)	0.4562
5	Center radius of core (3)	1.1329
6	In next assembly to control rods (1)	0.7744
7	In assembly beside reflector (3)	1.2929
Excore 1 and 2	In reflector (3)	1.20

^aApproximate distance in unit of assembly (23.6 cm flat to flat).

^bRatio of the detection rate of a 1/v detector with and without the control rods. [See Eq. (3)].

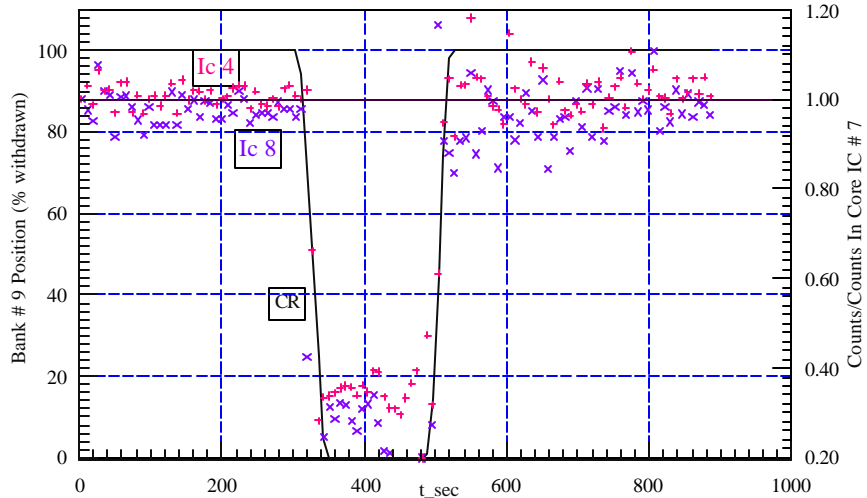


Figure 2. Control rod positions and ratio of counting rates as a function of time. The signals from all detectors are normalized to one at time 0, then the signals from detectors 4 and 8 are divided by the signal from detector 7.

The detector rates were calculated with the quasistatic method, with the following initial and final normalization: (1) the reactivity of the initial state (a few cents) was defined by the experimental period (an observable) and the inhour equation (which depends on the set of delayed parameters), this reactivity was added to the reactivity corresponding to the bank No. 9 totally inserted (which is a calculated value); and (2) the joining function for the interpolation between the two reactivity values [$\cos^2(\pi H_{cr}/2 H_{c_{ef}})$, where H_{cr} is the position of the bottom of the rod with respect to the bottom of the core, and $H_{c_{ef}}$ is an effective core height] was iterated in $H_{c_{ef}}$ until the measured value of excore detector 1 at end of the transient was found. A value $H_{c_{ef}} = 260$ cm (comparable to the 237-cm core height) for transients calculated with ENDF/B-V delayed parameters produces excellent results for all detectors. Figure 3 shows the case for the detectors more affected by the transient (4 and 8 located in the assembly with the control rods).

The calculations shown in Figure 3 correspond to the ENDF/B-V delayed neutron data with adjustment parameters $\beta_V = 5.56$ c for the initial reactivity and $H_{c_{ef}} = 260$ cm for the joining function; ENDF/B-VI data would have produced similar results but with $\beta_{VI} = 4.92$ c and a shorter $H_{c_{ef}}$.

CONCLUSIONS

Transients generated by the movement of control rods in a full mock-up of a VVER-1000 reactor at beginning of life and cold conditions were analyzed with a quasistatic model. The comparison of the results with measured signals from several detectors (including detectors in the assemblies with the control rods) shows very good agreement. Effective delayed parameters are determined primarily by the relative fission productions between U isotopes, rather than the differences between the spectra of prompt and delayed neutrons. The analysis is sensitive to differences in the reactivity scale between ENDF/B-V and VI delayed neutron nuclear data. Recent measurements¹⁰ of the delayed neutron activity in ²³⁵U agree better with Keepin's and ENDF/B-V data. The studies presented here support the conclusion that American reactor physics programs and data libraries can be used to analyze control rod withdrawal transients in partially MOX-fueled VVERs.

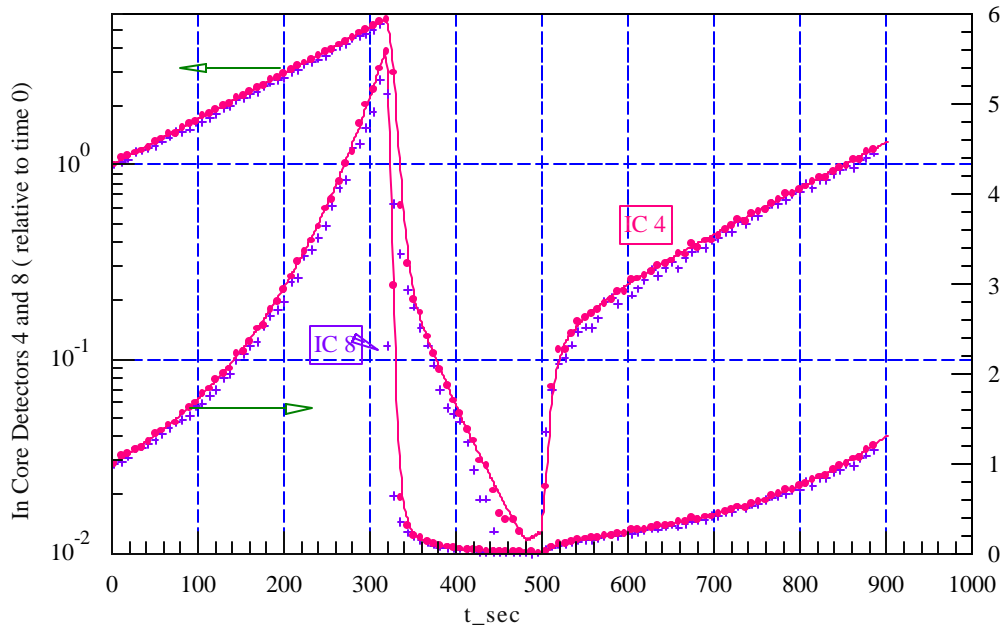


Figure 3. Measured and calculated signals from incore detectors 4 and 8 located in equivalent assemblies with control rods.

ACKNOWLEDGMENTS

This research was sponsored by Fissile Materials Disposition Program and performed at Oak Ridge National Laboratory, managed by Lockheed Martin Energy Research Corp., for the U.S. Department of Energy under contract DE-AC05-96OR22464.

REFERENCES

1. A. M. Pavlovitchev et al., Kurchatov Institute, "Documentation of Removal Transient Conducted at Kurchatov Institute Using an Array of LEU VVER-1000 Typical Fuel Assemblies," personal communication to R. T. Primm (ORNL), Moscow 1998.
2. F. C. Difilippo "LEU-HTR PROTEUS: Theory and Simulations of Reactivity Measurements with the Inverse Kinetics Methods," PSI TM-41-91-38, Switzerland, April 27, 1992. See also "Analysis of Kinetics Experiments in LEU-HTR Configurations of the PROTEUS Facility," TANS, **65**, 457-459 (1992).
3. N. M. Greene, W. E. Ford III, L. M. Petrie, and J. W. Arwood, *AMPX-77: A Modular Code System for Generating Coupled Multigroup Neutron-Gamma Cross Section Libraries from ENDF/B-IV and/or ENDF/B-V*, Oak Ridge National Laboratory, ORNL/CSD/TM-283 (October 1992).
4. J. J. Casal, R. J. J. Stamm'ler, E. A. Villarino, and A. A. Ferri, "HELIOS: Geometric Capabilities of a New Fuel-Assembly Program," *Proc. Int. Topl. Mtg. Advanced in Mathematics, Computations, and Reactor Physics, Pittsburgh, Pennsylvania, April 28-May 2, 1981*, Vol. 2, p.10.2.1-1.
5. DOORS, Version 3.1. See Web page <http://epmnas.epm.ornl.gov/home.html>.

6. D. R. Vondy, T. B. Fowler, and G. W. Cunningham III, *The Bold Venture Computation System for Nuclear Reactor Core Analysis, Version III*, Oak Ridge National Laboratory, ORNL-5711 (June 1981).
7. G. R. Keepin, T. F. Wimet, and R. K. Zeigler, "Delayed Neutrons from Fissionable Isotopes of Uranium, Plutonium, and Thorium," *J. Nucl. Energy*, **6**, 1 (1957).
8. J. C. Ryman, Oak Ridge National Laboratory, personal communication (October 1999).
9. A. C. Hindmarsh, "ODEPAK, A Systematized Collection of ODE Solvers," Scientific Computation, R. S. Stepleman et al. (eds.), North-Holland, Amsterdam, pp. 55–64 (1983).
10. D. J. Loaiza, G. Brunson, R. Sanchez, and K. Butterfield, "Measurements of Absolute Delayed Neutron Yield and Group Constants in the Fast Fission of ^{235}U and ^{237}Np ," *Nucl. Sc. and Eng.*, **128**, 270–277 (1998).